

Low Energy ACR Beyond the Termination Shock as a Source of Energetic Neutrals: Models and Observations

A. Czechowski¹, H. Fichtner², S. Grzedzielski³, M. Hilchenbach⁴, K.C. Hsieh⁵, J.R. Jokipii⁶, T. Kausch⁷, J. Kota⁶ and A. Shaw⁵

¹Space Research Centre, Polish Academy of Sciences, Bartycka 18A, 00-719 Warsaw, Poland

²Institut für Theoretische Physik IV, Ruhr-Universität Bochum, D-44780 Bochum, Germany

³Service d'Aeronomie du CNRS, B.P. No 3, Verrieres le Buisson, F-91371, France

⁴Max-Planck-Institut fuer Aeronomie, Max-Planck-Str. 2, Katlenburg-Lindau, D-37191, Germany

⁵Department of Physics, University of Arizona, Tucson AZ 85721, U.S.A.

⁶Lunar and Planetary Laboratory, University of Arizona, Tucson AZ 85721, U.S.A.

⁷Institut für Astrophysik und Extraterrestrische Forschung, Universität Bonn, Auf dem Hügel 71, D-53121 Bonn, Germany

Abstract

Observations by CELIAS/HSTOF on SOHO of the neutral flux in the 55-80 keV energy range, with the highest flux coming from the LISM anti-apex direction, are compared with model calculations which assume that the neutral flux originates, by charge-exchange with the background neutral gas of LISM origin, from the low energy ACR particles beyond the heliospheric termination shock. Different models of the outer heliosphere are taken as a basis of calculations and the effect on the resulting ACR density distribution and the flux of ENA is estimated. The viability of using the ENA as a means of imaging the structure of the termination shock, the distant heliosphere and the VLISM is discussed.

1 Introduction:

The flux of 55-80 keV mass=1 particles observed by CELIAS/HSTOF on SOHO, during quiet times in 1996 and 1997, was interpreted by Hilchenbach et al. (1998) as that of hydrogen atoms converted from anomalous cosmic-ray (ACR) protons in the outer heliosphere, as anticipated by Hsieh et al. (1992). The peaking of the flux during periods, when the instrument was viewing the anti-apex direction of the heliosphere with respect to the local interstellar medium (LISM), coincides with the anisotropy predicted by Czechowski, Grzedzielski and Mostafa (1995) and Czechowski and Grzedzielski (1997) based on the simulations of the production of ENA from ACR, when the transport of ACR in the heliosheath is taken into account. The regions of interest and the subjects of discussion here are schematically shown in Figure 1.

While not yet confirmed by direct observations, the model simulations (Bara-

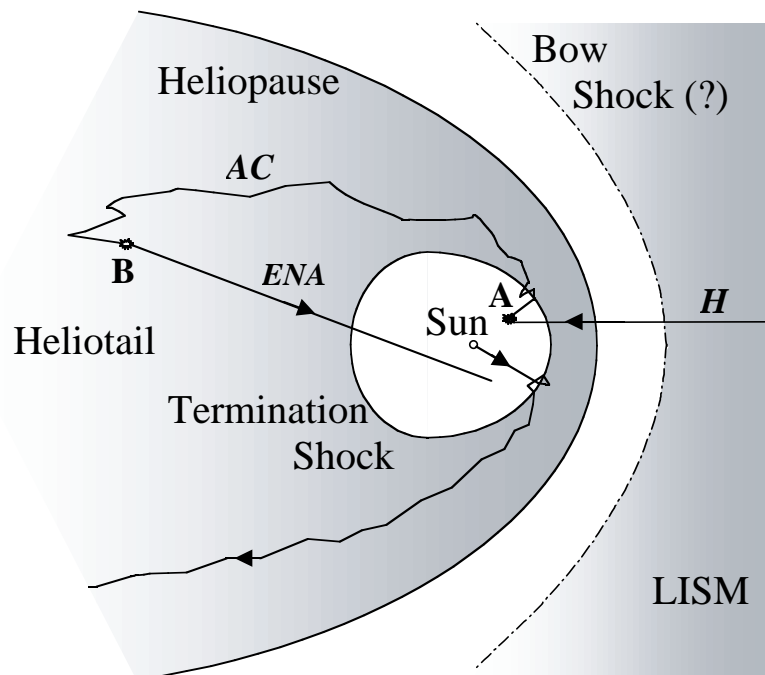


Figure 1: A view of the heliosphere: ACR conversion to ENA is shown.

nov & Malama, 1993, Zank et al., 1996, Linde et al., 1998, Ratkiewicz et al., 1998) of the interaction between the solar wind and the LISM plasmas, in agreement with the pioneering work by Parker (1963), result in picture of the heliosphere in which the plasma flow outside the termination shock, at which the solar wind decelerates, develops a stagnation point towards the LISM apex and a long wake (the heliotail) towards the anti-apex. The solar plasma is separated from the LISM plasma by the heliopause which can, however, be crossed by the neutral atoms from the LISM. Their charge-exchange interaction with the plasma ions, which converts the neutrals into pick-up ions and the plasma ions into neutral solar wind particles, affects significantly the structure of the heliosphere and the near LISM (Baranov and Malama, 1996).

The termination shock is the probable source of ACR by acceleration of solar-wind ions, particularly the pick-up ion component. Low-energy ACR (small coefficient of diffusion) cannot penetrate far upstream of the shock, but will instead be convected downstream with the solar plasma into the heliotail. At low energies, the transcharging of the ACR with the ambient neutral gas of LISM is especially favored due to larger cross sections (Shih, 1993). The model calculations of the spatial distribution of ACR downstream of the termination shock (Czechowski, Grzedzielski and Mostafa, 1995; Czechowski and Grzedzielski, 1997) suggest that the low-energy ACR will concentrate in the heliotail region, which implies that the maximum flux of ENA of ACR origin should arrive from the anti-apex (heliotail) direction.

Observations of ENA may provide the means for imaging the distribution of ACR in the distant heliosphere, which reflects both the global structure of the heliosphere and the ACR generation mechanism. To assess the possibilities of this approach we combine in the present contribution the calculations of the distribution and modulation of the ACR spectrum based on a model of the heliosphere that is more realistic than those used in the past, with a discussion of the ENA data. For the general information on the production of energetic neutral atoms (ENA) and their presence in interplanetary space, we refer to paper SH 2.2.01.

The evolution of ACR energy spectrum is discussed in paper SH 4.3.01. Another related topic is the contribution to ENA from the pre-accelerated pick-up ion population in the heliosphere, which is considered in paper SH 4.1.03.

2 Basic Theory of Transport and Acceleration of ACR:

The anomalous component of cosmic rays is composed of fluxes of helium, nitrogen, oxygen, neon, protons and low levels of carbon, which are observed to be enhanced in a region of the energy spectrum ranging from a kinetic energy of ~ 20 MeV to 1.6 GeV. The radial intensity gradient is positive out to the maximum distance reached by current spacecraft, indicating that this component probably originates by acceleration at the solar-wind termination shock. This shock is quasi-perpendicular over most of its area, so the acceleration involves drift along the shock face (Jokipii, 1982, 1987). The transport equation for the pitch-angle-averaged distribution function $f(\mathbf{r}, p, t)$ as a function of position \mathbf{r} , particle momentum p , and time t , may be written (see, e.g., Parker, 1965) as

$$\frac{\partial f}{\partial t} = \frac{\partial}{\partial x_i} \left[\kappa_{ij}^{(s)} \frac{\partial f}{\partial x_j} \right] - \mathbf{V} \cdot \nabla f - \mathbf{V}_d \cdot \nabla f + \frac{1}{3} \nabla \cdot \mathbf{V} \left[\frac{\partial f}{\partial \ln p} \right] + Q \quad (1)$$

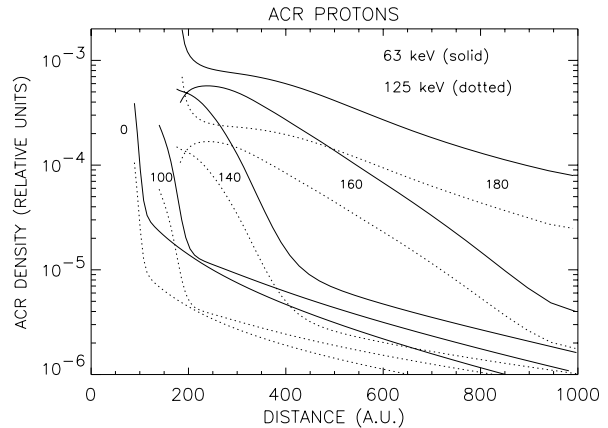


Figure 2: ACR proton distribution presented as constant θ (angle from the apex) density profiles plotted against distance from the Sun, for $\theta = 0, 100, 140, 160$ and 180 deg.

where the successive terms on the right-hand side correspond to diffusion, convection, particle drift, adiabatic cooling or heating and any local source Q . Here, the drift velocity in the magnetic field \mathbf{B} is $\mathbf{V}_d = pcw/3q \nabla \times [\mathbf{B}/B^2]$ where c is the speed of light, w the speed of the particle and $\kappa_{ij}^{(S)}$ is the symmetric part of the diffusion tensor.

We are here interested in the very lowest-energy accelerated particles. For those, the diffusion is quite slow, and we may approximate the accelerated spectrum with that obtained from simple planar-shock theory. That this is reasonable is readily seen by noting that the relevant diffusion scale κ/V is much less than the macroscopic length scales, which are of the order of tens of AU. For a locally planar shock, it is a simple matter (see, e.g., Drury, 1983) to show that the accelerated particles have the spectrum $f(p) \propto (1/\Delta V)p^{-q}$ where ΔV is the change of the velocity normal to the shock, at the shock, and where $q = 3r_{sh}/(r_{sh} - 1)$.

In the region downstream from the shock the magnetic field must lose the regularities typical for the inner region. At larger distance scales, assuming disordered field structure may be a reasonable approximation. We replace the diffusion tensor by a scalar coefficient: $\kappa\delta_{ij}$ which also implies disregarding the drifts (which would not have a strong effect in the low energy range). The diffusion coefficient in the LISM (outside the heliopause) is taken to be much larger (a factor of 10^2) than inside. In the transport equation, the charge-exchange loss term of the form $\beta_{cx}f$ will be an important contribution.

3 ENA produced by ACR: Model Results

Our calculations consist in solving the transport equation for the distribution of ACR in the region outside of the termination shock, assuming a given model of the heliosphere (which determines the plasma flow, the diffusion coefficient and the charge-exchange loss rate). The associated flux of ENA is given by a line integral of the ACR flux $j_{ACR} = p^2 f(\mathbf{r}, p, t)$ weighted by the charge-exchange cross section, the neutral density and the extinction factor. The scale of the ACR flux intensity at the shock, which sets the boundary condition for our simulation, is obtained by matching with the shock spectrum of Stone, Cummings and Webber (1996). Figure 2 shows the shape of the spatial distribution of ACR protons outside the termination shock for two values of energy: 63 keV and 125 keV. The variation of the ACR energy spectrum (slope and amplitude) over the surface of the shock, reflecting the variation of the shock strength and of the upstream flow speed, is taken into account in this simulation (the previous calculations assumed a fixed shock spectrum). These variations are smoothed out within $\sim 10^1$ A.U. downstream from the shock. The concentration of the ACR particles in the heliotail is clearly seen. The heliopause, at which the diffusion coefficient is assumed to change to a higher value, corresponds to an abrupt change in the slope of the density profiles.

The results for the ENA flux are illustrated in Fig. 3 (the case of fixed shock spectrum) including those

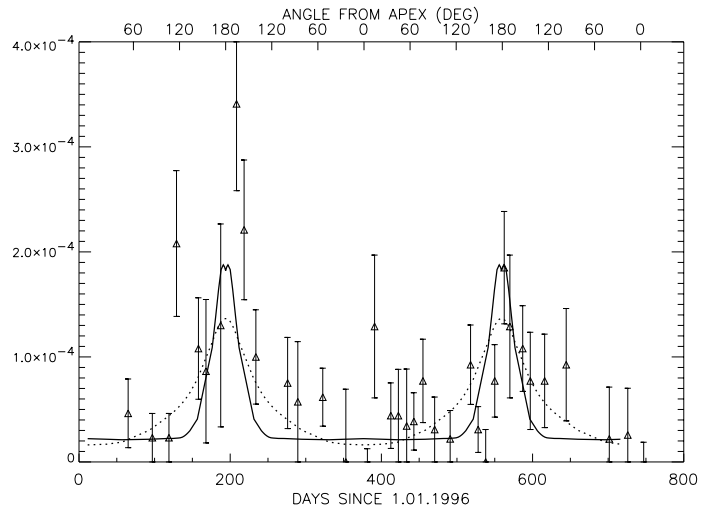


Figure 3: ENA flux: the data points show the flux (units $(cm^2 s sr keV)^{-1}$) of mass=1 particles in low energy channels ($\sim 55-80$ keV) observed during quiet times (low ion flux) by CELIAS/HSTOF instrument. The calculated flux of 63 keV hydrogen ENA from ACR transcharging in the field of view of the instrument is shown for the cases of Kausch's (solid line) and Parker's (dotted) models of the heliosphere.

obtained in a simplified model based on Parker's analytical solution for the heliospheric flow (Parker 1963). The model we use in present calculations (Kausch, 1998) has the density of the background hydrogen in the heliotail significantly lower (0.02 cm^{-3}) than in the LISM. Also, there is a hydrogen wall in front, outside of the heliopause. Nevertheless, the flux comes predominantly from the heliotail direction. The intensity peak is about 60 degrees wide, corresponding to about 60 days of CELIAS/HSTOF observations. For the case of Parker's model we assumed the neutral hydrogen density $=0.1 \text{ cm}^{-3}$ inside the heliopause. The Kausch simulation used here assumed $n_H = 0.1 \text{ cm}^{-3}$ in the LISM, which may be low (Lallement et al. 1991). Charge exchange of ACR protons with neutral helium, which is not appreciably depleted in the heliotail region (we assume $n_{He} = 0.01 \text{ cm}^{-3}$) is then an important ($\sim 30\%$) contribution.

4 Discussion

In the calculations reported here, the ACR distribution beyond the termination shock was for the first time treated using a reasonably realistic model of the heliosphere, which incorporates the very important interaction with neutral background. In particular, the calculations included the non-spherical termination shock, with parameters varying over the surface, and the effect of adiabatic energy changes in a $\nabla \cdot \mathbf{V} \neq 0$ plasma flow. The prediction of the anisotropy of the ENA flux (highest flux from the anti-apex) was confirmed. The shape of the ENA intensity peaks can be seen to depend on the details of the model.

The intensity scale of the calculated ENA flux is in a reasonable agreement with observations. In the data from CELIAS/HSTOF the intensity of the ENA flux at the 1996 peak is larger by a factor of 1.5 than the corresponding peak in 1997. This cannot be explained by a variation in the conditions at the lower boundary (the shock) because of low plasma speed downstream. The further data analysis (which is in progress) is needed to clarify the situation.

References

- Baranov, V.B. & Malama, Yu.G. 1993, *Journ. Geophys. Res.* 98, 15157
 Czechowski, A., Grzedzielski, S. & Mostafa, I. 1995, *A&A* 297, 892
 Czechowski, A. & Grzedzielski, S. 1997, *Proceedings of the 25th ICRC, Durban 1997*
 Drury, L. 1983, *Rpt. Prog. Phys.* 46, 973
 Hilchenbach, M., Hsieh, K.C., Hovestadt, D. et al. 1998, *ApJ* 503, 916
 Hsieh, K.C., Shih, K.L., Jokipii, J.R. & Grzedzielski, S. 1992, *ApJ* 393, 756
 Jokipii, J.R. 1982, *ApJ* 255, 716
 Jokipii, J.R. 1987, *ApJ* 313, 842
 Kausch, T. 1998, Ph.D. Thesis (Univ. of Bonn)
 Lallement, R., Bertaux, J.-L., Chassefiere, E., Sandel, B. 1991, in: *Physics of the Outer Heliosphere, COSPAR Coll. Vol.1*, eds. Grzedzielski, S. & Page, D.E. (Pergamon, Oxford), p.73
 Linde, T.J., Gombosi, T.I., Roe, P.L., Powell, K.G. & DeZeeuw, D.L. 1998, *Journ. Geophys. Res.* 103, 1889
 Parker, E.N. 1963, *Interplanetary Dynamical Processes* (Interscience, New York)
 Parker, E.N. 1965, *Planet. Space Sci.* 13, 9
 leRoux, J.A., Potgieter, M.S. & Ptuskin, V.S. 1996, *Journ. Geophys. Res.* 101, 4791
 Ratkiewicz, R., Barnes, A., Molvik, G.A., Spreiter, J.R., Stahara, S.S., Vinokur, M., Venkateswaran, S. 1998, *A&A* 335, 363
 Shih, K.-L., 1993, Ph. D. thesis (Univ. of Arizona)
 Stone, E.C., Cummings, A.C. & Webber, W.R. 1996, *Journ. Geophys. Res.* 101, 11017
 Zank, G.P., Pauls, H.L., Williams, L.L. & Hall, D.T. 1996, *Journ. Geophys. Res.* 101, 21639